Enhancement of the photovoltaic performance in P3HT: PbS hybrid solar cells using small size PbS quantum dots

Yuliar Firdaus[1], Erwin Vandenplas[2], Yolanda Justo[3], Robert Gehlhaar[2], David Cheyns[2], Zeger Hens[3], Mark Van der Auweraer[1,a)]

[1] *Laboratory of Photochemistry and Spectroscopy, Division of Molecular Imaging and Photonics, Chemistry Department, KULeuven, Celestijnenlaan 200F, 2404, B-3001 Leuven, Belgium*

[2] *Imec vzw, Kapeldreef 75, B-3001 Leuven, Belgium*

[3] *Physical Chemistry Laboratory, Ghent University, Krijgslaan 281-S3, 9000, Gent, Belgium*

Abstract

Different approaches of surface modification of the quantum dots (QDs), namely solution-phase (octylamine, octanethiol) and post-deposition (acetic acid, 1,4-benzenedithiol) ligand exchange, were used in the fabrication of hybrid bulk heterojunction solar cell containing poly (3-hexylthiophene) (P3HT) and small (2.4 nm) PbS QDs. We show that replacing oleic acid (OLA) by shorter chain ligands improves the figures of merit of the solar cells. This can possibly be attributed to a combination of a reduced thickness of the barrier for electron transfer and an optimized phase separation. The best results were obtained for post-deposition ligand exchange by 1,4 benzenedithiol (BDT) which improves the power conversion efficiency of solar cells based on a bulk heterojunction of lead sulfide (PbS) QDs and P3HT up to two orders of magnitude over previously reported hybrid cells based on a bulk heterojunction of P3HT:PbS QDs where the QDs are capped by acetic acid ligands. The optimal performance was obtained for solar cells with 69 wt% PbS QDs. Besides the ligand effects the improvement was attributed to the formation of an energetically favorable bulk heterojunction with P3HT when small size (2.4 nm) PbS QDs were used. Dark current density-voltage (*J-V*) measurements carried out on the device provided insight into the working mechanism: the comparison between the dark *J-V* characteristics of the bench mark system P3HT:PCBM and the P3HT:PbS blends allows us to conclude that a larger leakage current and a more efficient recombination are the major factors responsible for the larger losses in the hybrid system.

[a)] Author to whom correspondence should be addressed. Electronic mail: mark.vanderauweraer@chem.kuleuven.be.

Keywords:

Hybrid solar cells; bulk-heterojunction solar cells; polymer; quantum-dots; PbS; ligand-exchange

I INTRODUCTION

Hybrid solar cells based on blends of semiconducting polymers and colloidal semiconductor nanocrystals (NCs), such as CdSe, CdS, CdTe, PbSe and PbS,[1] have attracted increased attention since the advantages of both classes of materials can be effectively combined. This concerns on one hand the size dependent and thus adjustable absorption properties of the quantum dots (QDs) and on the other hand the ease of processing of the two materials from solution and the potential for making low-cost solar cells with reasonable stability. Among the different semiconductor NCs under investigation for photovoltaic applications, PbS QDs have emerged as one of the most promising candidates due to their high electron mobility [2], tunable and broad absorption in the near-infrared [3], carrier multiplication [4] and stability in air [5]. However, despite of the advantages, most of photovoltaic devices fabricated from mixtures of PbS QDs and traditional conjugated polymers showed a much lower power conversion efficiency (PCE) ranging from 0.0013% to 0.7% [6,7] than the analogous polymer:CdSe blends where a PCE up to 2.9% was found [8]. Notable exceptions are PbS-based photovoltaic devices where the PbS QDs are mixed with a narrow band-gap polymer [9–11].

It has been suggested that the low photovoltaic performance of poly(3-hexylthiophene) (P3HT):PbS(PbSe) hybrid devices is primarily due to a lack of photo-induced charge transfer at the organic/inorganic interface.[10–13] Therefore, the ligands surrounding the QD surface can play a critical role as they can potentially influence both the morphology and several photophysical processes ranging from exciton diffusion to charge generation and extraction. On one hand, in order to achieve an efficient photo-induced charge transfer and charge transport it is necessary to replace the long ligands, present on the QDs after synthesis, with shorter ones. On the other hand, capping the QDs with short ligands can lead to clustering of the exchanged QDs and can limit their solubility. The morphology of the hybrid blends has to provide a high interface area for exciton dissociation and simultaneously a continuous transport pathway for both holes and electrons to respectively the cathode and the anode. In this regard, the ligand exchange process is

challenging since often the increased clustering and limited solubility of the exchanged QDs result in a more extensive phase separation and higher surface roughness [1].

Hyun *et al.* [14] reported that upon decreasing the size of PbS QDs the increase of the band gap is accompanied by both a rise of the lowest unoccupied molecular orbital (LUMO) level and a decrease of the energy of the highest occupied molecular orbital (HOMO) level. Therefore, a decrease of the size of PbS QDs is expected to give a better energy-level alignment with P3HT leading to a smaller energy loss in the charge generation step (and hence a larger V_{oc}) and a more exergonic and hence slower charge recombination, as the latter process is expected to be in the Marcus inverted region[15,16] in P3HT:PbS hybrid solar cell system. Furthermore, using QDs of smaller size will allow one to get, for the same load of QDs, a higher number density and hence a smaller average distance from the P3HT chromophores to the QDs, resulting in more efficient exciton dissociation. When replacing the oleic acid (OLA) ligands, present on commercially available QDs or QDs synthesized with a standard procedure, with tailored ligands, the miscibility and efficient electrical coupling of the nanocrystals with their surrounding environment should be considered in order to achieve a noticeable enhancement of the photovoltaic performance. Zhang *et al.* [17] have shown that treating the PbS QDs with octylamine, (OAm) in order to achieve a solution-phase ligand exchange, improved the efficiency of a device based on a blend of MEH-PPV and PbS QDs compared to devices fabricated from OLA-capped QDs. The development of colloidal QD solar cells has benefitted further from post-deposition ligand exchange by thiols which was used in order to avoid excessive aggregation of the PbS QDs which occurred when the ligand exchange was performed in solution [18].

Moreover, Seo *et al.* [19] previously reported an improvement of photovoltaic performance (energy efficiency (PCE)) of a P3HT/PbS device to 0.01% employing post-deposition ligand exchange using short-length ligands as acetic acid. Post-deposition ligand exchange with bifunctional linker molecules such as ethanedithiol and 1,4 benzenedithiol have also been used recently [9,10,20]. These treatments have improved the energy efficiency of narrow-gap polymer:PbS blends up to ~3% [9], which approaches typical values of P3HT:PCBM solar cells [21] but is still a factor of two to three below the best values of solar cells based on low band gap polymers and PCBM [22–24]. The improved efficiency was attributed to an increased mobility and a decreased recombination loss [9].

In the study reported here, we demonstrate the fabrication of hybrid solar cells using a P3HT polymer and small size PbS QDs. The performance of the photovoltaic devices for different QD concentrations and surface modification treatments of the QDs are presented. Octylamine (OAm) and octanethiol (OT) were used as short-length ligands for the solution phase ligand exchange while acetic acid (AA) and 1,4-benzenedithiol (BDT) were used for the post-deposition ligand exchange. By fitting the measured dark current density-voltage (*J-V)* characteristics of the solar cells, we were able to extract various diode parameters including the saturation current and to examine the effect of ligand exchange process and the concentration of PbS QDs on the dark *J-V* characteristics. The obtained results will be compared with following bench mark systems: a bulk-heterojunction of P3HT:PbS QDs capped with AA ligands [19] and a bulk-heterojunction of P3HT:PCBM [21].

II EXPERIMENTAL

A **Materials**

The colloidal PbS QDs with a core diameter of approximately 2.4 nm and capped by OLA were purchased from Evident Technologies (Troy, NY). PbS QDs of 3.5 and 4.4 nm size (capped with OLA) were obtained from Ghent University. The synthesis of PbS QDs (3.5 nm and 4.4 nm) is described in detail in Ref. [25] and [26]. P3HT was obtained from Rieke Metals under the commercial name Sepiolid P200 (Number-average molecular-weight = 13.9 kg/mol, polydispersity = 1.71, regioregularity > 96%).

B Solution-phase ligand exchange

Ligand exchange from the OLA to the OAm ligand was performed by adding OAm to a solution of the QDs in toluene (1:1 by volume). After storing the mixture for three days without stirring in a nitrogen environment, methanol was added to precipitate the PbS QDs which were redispersed in chlorobenzene. As exchange of OLA (X-type ligands) by OAm ligands (L-type ligands) is not evident and not completely understood [27–29], the ligand exchange was checked by IR and NMR spectroscopy. The FTIR spectra show after ligand exchange a reduced intensity or even complete disappearance of the CH stretching mode near 3025 cm^{-1} suggesting a displacement, or removal, of most oleate groups from the QD surface while the appearance of a band at 3068 cm^{-1} is attributed to the NH-stretching of amine ligands bound to the PbS surface [30].

The ^{1}HNMR experiments confirmed that the OLA ligands were removed and replaced for 40% by amine ligands [31]. Also HRTEM imaging suggested that ligand exchange to octylamine induced the fusion of QDs to nanorods consisting of three to four individual QDs [30,31].

For the OT ligand exchange, an excess of OT (1:1 by volume) was added to a solution of PbS QDs, mixed in a glass tube and heated using a heat gun for about 5 minutes. A mixture of the non-solvents isopropanol and methanol (2:1 by volume) was then added to precipitate the solution and the sample was centrifuged. The PbS QDs were then redispersed in chloroform followed by washing once with the non-solvent mixture to remove the remaining free ligands.

C Post-deposition ligand exchange

The post-deposition ligand exchange allow direct chemical ligand replacement in a blended mixture of P3HT:PbS-OLA.[9,19] The ligand exchange was carried out by soaking the blend film of P3HT:PbS-OLA (*cfr.infra*) in a 0.1 M solution of AA or 0.02 M BDT in acetonitrile for 60 s followed by spinning the substrate at 1000 rpm for 30 s to remove the solvent and any residual AA or BDT.

D Device fabrication

The cells were prepared on glass/ITO substrates. First the substrates were pre-cleaned in an ultrasonic bath with Hellmanex detergent, deionized water, acetone and isopropanol, and treated in an ultraviolet-ozone chamber for 30 minutes. A thin layer (~30 nm) of poly(3,4-ethylenedioxythiophene):poly(styrene sulfonate) (PEDOT:PSS, Baytron P VP AI 4083) was spin-coated 3500 rpm for 60 s onto the ITO glass and then baked at 150°C for 15 minutes.

A blend of P3HT:PbS QDs (60, 75 and 90 % loading of QDs) was dissolved in chloroform or chlorobenzene at a concentration of 20 mg/ml (PbS core and P3HT). The loading by QDs corresponds to the weight of PbS divided by sum of the weight of PbS and P3HT as these parameters could be determined unambiguously from the preparation of the solution. The actual weight fraction of PbS in the film will be significantly smaller as also the mass of the ligands has to be considered (see supporting information (SI)[32]). OAm- and OT-capped QDs were mixed immediately with P3HT after the ligand exchange and stirred at 70°C for 15 minutes. The blend solutions were spin-coated (1000 rpm for 60 s) on the PEDOT:PSS layer to form a

photosensitive layer. For post-deposition ligand exchange, P3HT was mixed with OLA-capped QDs for at least 2 hours at 70°C before being spin-coated (1000 rpm for 60 s) on the PEDOT-PSS layer. This was followed by the ligand exchange as described in section 2C. All the films were subsequently annealed at 150°C for 10 minutes inside a nitrogen-filled glove box. Finally, the device fabrication was completed by the thermal evaporation of Ca (~20 nm) and Ag (100 nm) as a cathode. Besides the devices with P3HT:PbS bulk-heterojunctions, we also produced a control device with a bulk-heterojunction of P3HT:PCBM with 50 wt % of PCBM.

E Electrical characterization of devices

Photovoltaic devices are measured inside a glove box with a parameter analyzer (Agilent 4156C) or a Keithley 2602A under a 1000W Xe arc lamp equipped with filters to simulate the AM 1.5G spectrum (Abet). The lamp is calibrated using a Fraunhofer calibrated Si solar cell, equipped with a band pass filter.

III RESULTS AND DISCUSSION

A P3HT:PbS solar cells

Fig. 1(a) shows the absorption spectrum of a PbS QDs-only film spin coated from a solution of OLA-capped PbS QDs in chlorobenzene which shows a characteristic first excitonic peak at 1.6 eV. This peak is slightly red-shifted compared to the absorption spectra of the PbS QDs dispersed in toluene as shown in Fig. S1 [32]. The absorption spectrum of a pristine P3HT film spin-coated from chlorobenzene shown in Fig. 1(a), covers in agreement with literature the range from 400 to 700 nm [33,34]. Using P3HT as an electron donor and PbS QD as an electron acceptor material, we fabricated a simple hybrid bulk heterojunction solar cell device. The estimated energy band diagram of the resulting device structure can be seen in Fig. 1(b). The estimated positions of the energy levels of the polymer and the PbS QDs were taken from Ref. [35] and [36], respectively. The estimated energy levels suggest the formation of an energetically favorable type-II heterojunction in the P3HT:PbS blends.

Ideally, in order to obtain a continuous transport pathway for each type of charges to their respective electrodes, the percolation threshold should be attained for the PbS QDs in the P3HT matrix [37]. According to the percolation theory the formation of interconnected paths of small

spherical molecules or particles embedded in a three dimensional matrix occurs at a volume fraction of 17% [37]. This means that for PbS QDs without capping ligands, the percolation threshold of the P3HT:PbS blend would be situated at almost 60 wt% of PbS QDs (which corresponds to 17 % vol). Taking into account the volume occupied by the ligands this would correspond to a loading of 65 % for QDs capped with AA to 82 % for QDs capped with OT. For QDs capped with OLA the percolation threshold would not be reached even for a loading of 100 % where the volume % of PbS QDs is still only 14.7 %. Therefore, the hybrid solar cell devices in this work were made with a loading of 60, 75 and 90 of PbS QDs (see Table S1[32]).

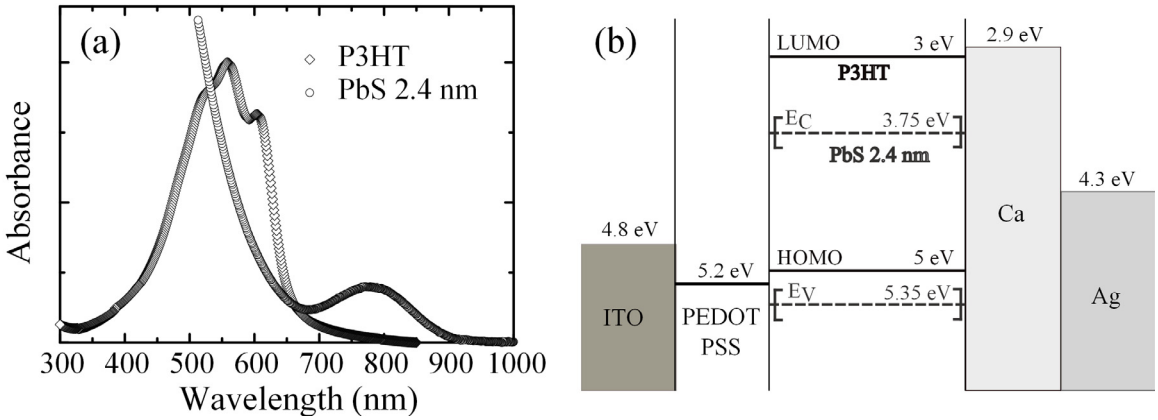

FIG. 1. (a) Absorption spectra of neat P3HT and PbS QDs (capped by OLA) films, (b) energy band diagram of the solar cell device structure fabricated in this work.

The difference of the concentrations expressed in weight and volume fraction in Table S1[32] is due to the large density of PbS.

To study the solar cell performance of the P3HT:PbS blends, *J-V* characteristics of the devices were measured under AM1.5G illumination at 100 mW/cm^2. The J_{sc} of the P3HT:PbS-OAm (60 % loading) device is almost two order of magnitudes larger than that obtained for a device with comparable thickness and loading where the QDs are capped with OLA, *i.e.* without ligand exchange (see Table I). However, the low V_{oc} and FF resulted in an overall PCE of only 0.002%. The increase of the PbS-OAm loading to 75 and 90 % further decreased the J_{sc} although a significant increase of V_{oc} resulted in a PCE of 0.0035%. We have shown that ligand exchange of PbS QDs with OAm induced a structural change of individual QDs which tends to form nanorods [30]. As thiol ligands are expected to bind stronger to the PbS surface than amines or

carboxylic acids we expected that less loss of ligands and QD aggregation would occur with the latter ligand. Hence we also tried to perform ligand exchange to OT ligands. For example, at 75 % loading of PbS-OT QDs, the overall PCE of the device with 140 nm thickness improved to 0.022%. In the device with a thickness of 100

TABLE I. Average photovoltaic performance values of P3HT:PbS blends. t, J_{SC}, V_{OC}, FF and PCE are respectively the thickness of the active layer, the short circuit current, the open-circuit voltage, the fill factor and the energy efficiency. (Values in the brackets are the best values recorded). *: Integrated planar-bulk-heterojunction structure: ITO/PEDOT:PSS/P3HT(5-10 nm)/P3HT:PbS/Ca/Ag (*cfr. infra*)

Samples	Acceptor[a] loading	t (nm)	J_{sc} (mA/cm^2)	V_{oc} (V)	FF (%)	PCE (%)
P3HT:PbS-OLA	60	100	$(3\pm0.6)\times10^{-3}$	0.09±0.06	27±3.9	$(8.6\pm5.9)\times10^{-5}$
P3HT:PbS-OAm	60	100	0.3±0.03	0.03±0.01	22±4.7	$(2\pm1.4)\times10^{-3}$
	75	140	0.01±0.005	0.016±0.005	23±5	$(5\pm1)\times10^{-4}$
	90	140	0.03±0.005	0.43±0.2	29±2	$(3.5\pm2)\times10^{-3}$
P3HT:PbS-OT	60	90	1.8±0.13	0.05±0.02	25±2	0.025±0.01
	75	140	0.3±0.04	0.24±0.07	28±1	0.02±0.006
	90	100	1.2±0.45	0.2±0.08	27±1.5	0.06±0.02
P3HT:PbS-AA	60	110	0.55±0.13	0.17±0.06	27±1.5	0.024±0.016
	75	100	0.2±0.03	0.06±0.025	25±2.6	$(2\pm0.9)\times10^{-3}$
	90	90	1.6±0.32	0.02±0.01	21±7.5	$(8\pm7)\times10^{-3}$
P3HT:PbS-BDT	60	180	1.7±0.06	0.33±0.01	42±1.2	0.233±0.02
	75	160	5.6±0.3	0.31±0.05	31±1.1	0.525±0.1
	90	160	7.2±0.1 (7.2)	0.35±0.02 (0.37)	33±0.8(34)	0.84±0.05(0.91)
	100	140	5±0.5(5.6)	0.43±0.01(0.43)	28±0.6(28)	0.59±0.07(0.68)
	90*	140	6.9±0.2 (7.1)	0.41±0.01 (0.42)	33±0.5(34)	0.93±0.05(1)
P3HT:PCBM	50	100	6.9±0.1(6.9)	0.6±0.01(0.62)	65±1.1(67)	2.72±0.1 (2.86)

[a]The acceptor loading corresponds to the ratio of the weight of PbS QDs to the sum of the weight of PbS QDs and P3HT

nm and with a PbS QD (with OT capping) loading of 90 % a further increase of the PCE to 0.055% (V_{oc}=0.18 mV; J_{sc}=1.2 mA/cm^2; FF=27%) (see Table I) was observed which is five times higher than the PCE that was reported previously for the bench mark system with a bulk-heterojunction of P3HT:PbS QDs capped with AA.[19] On the other hand, post-deposition ligand

exchange on P3HT:PbS-OLA blend films using 0.02 M AA resulted in an average PCE of 0.024%, 0.002% and 0.008% for a PbS QDs loading of 60, 75 and 90 % respectively and a film thickness around 100 nm (see Table I).

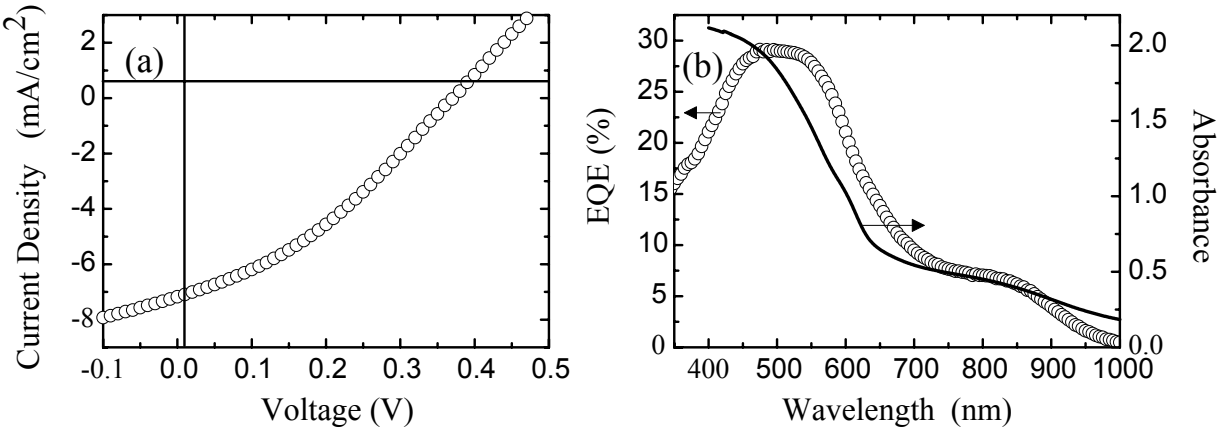

FIG. 2. (a) *J-V* characteristic of a P3HT:PbS-BDT (90 % loading) blend device (160 nm) under AM 1.5G (100 mW/cm^2) illumination. (b) Plots of the absorption spectrum of the P3HT:PbS-BDT (90 % loading) blend (solid line) and the External Quantum Efficiency (EQE) spectrum (◊) of the blend device with a thickness of 160 nm.

A further significant improvement of the solar cell performance was obtained when we performed the post-deposition treatment of the blend film containing PbS QDs capped by OLA using BDT (see Table I). The optimum performance was obtained for a PbS QDs with a loading of 90 % (corresponding to 69 wt % or 26 vol. % of PbS) and a thickness ~160 nm (see Table S3[32]). This device resulted in average PCE of 0.84% with the best value for the PCE of 0.91% (Fig. 2(a): J_{sc}=7.2 mA/cm^2, V_{oc}=0.37 V and FF=34.3%). This result corresponds to an improvement by almost two orders of magnitude compared to the best device based on a P3HT:PbS QD bulk-heterojunction reported up to now by Seo *et al.*[19] However the PCEs are still a factor of three to four below the typical values of 3.8 to 4 % reported for bulk heterojunctions of P3HT:PCBM [21] and of 3 % reported for low band gap polymers and PbS QDs [9]. Fig. 2(b) compares the external quantum efficiency (EQE) spectrum of the corresponding device of P3HT:PbS-BDT blends and the absorption spectrum of the blend film. The EQE of the device reaches 30% at 500 nm. The EQE spectra obtained from the device were consistent with the absorption spectra of the film. In the EQE spectrum, the major contribution from P3HT is in the range from 400-700 nm. However, one should note that the EQE extends to 1000 nm, primarily

due to excitonic absorption of the PbS QDs. This shows that light absorbed by both the P3HT polymer and the near-infrared absorbing PbS QDs contributes to the photocurrent.

The results shows the effectiveness of the short bi-dentate ligands such as BDT to replace the long insulating ligands, reducing the inter-particle spacing as well as the barrier for photo-induced electron transfer from the excited P3HT to PbS QDs or photo-induced hole transfer from excited PbS QDs to P3HT. The treatment may also increase the electronic coupling between QDs and eventually the transport properties as demonstrated in previous work [38]. A detailed transmission electron microscopy (TEM) and optical spectroscopy study, which will be published elsewhere[39], also showed that the BDT treatment led to a significant change in morphology, optical absorption and efficiency of the charge transfer process in the P3HT:PbS blend films.

B Dark current density-voltage characteristics

As the dark current density-voltage (*J-V*) characteristics of solar cells may provide useful information to analyze the performance losses and device efficiency [40] we also measured the dark *J-V* characteristics of P3HT:PbS solar cells. To investigate the variation in series resistance, shunt resistance, ideality factor, and saturation current, the dark current density was fitted by an equivalent circuit model including both a series and a shunt resistance[41]:

$$J = J_0\left[exp\left(\frac{q\left(V - JAR_s\right)}{nkT}\right) - 1\right] + \frac{V - JAR_s}{AR_{sh}} \qquad (1)$$

Where J_0 is the dark saturation current density (A/cm^2), R_s is the series resistance (Ω), R_{sh} is the shunt resistance (Ω), A is the device area (cm^2), and n is the ideality factor. First, this transcendental equation was solved iteratively using the Newton-Raphson method to give the current density at a given bias voltage. Next, the measured dark *J-V* data were fitted by minimizing (Levenberg-Marquardt algorithm [42]) the sum of the squared deviations between the data and the current density computed using equation (1). In order to increase the precision with which the different parameters were recovered we always took the average of data obtained for three different cells. The standard deviations on these data also give an estimate of the precision with which the parameters were recovered.

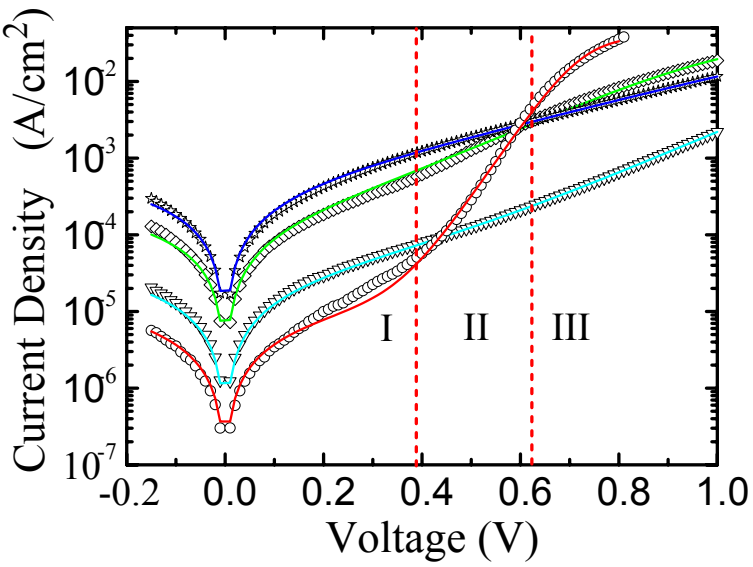

FIG. 3. Current density-Voltage (*J-V*) characteristics in the dark for the P3HT:PbS (capped with BDT) and the reference P3HT:PCBM solar cells with the structure of ITO/PEDOT:PSS/active-layer/Ca/Ag. The open symbols are the experimentally measured data, while the solid lines are fits according to an equivalent circuit model including series and shunt resistance (equation 1). The three regions separated by red dashed lines are indicated for the P3HT:PCBM solar cells where different effects dominate: region I determined by R_{sh}, region II by the diode parameters J_0 and n, and region III by R_s. □, ——: 90 wt% PbS, ◇, ——: 90 wt% PbS (integrated), ▽, ——: 100 wt% PbS, ○, ——: 50 wt% PCBM

As seen in Fig. 3, the solid lines are fitted curves, which are in good agreement with the measured data. The fitting variables: R_s, R_{sh}, J_0 and n for the P3HT:PbS solar cells are summarized in Table II. A typical dark *J-V* plot (semi-logarithmic scale) of the reference sample, a P3HT:PCBM 50 wt% solar cell, is also shown in Fig. 3. The three regions illustrate how the different components of the equivalent circuit of the solar cell dominate the features of the plots: At low voltages (region I), the *J-V* characteristics are primarily determined by leakage (shunt) currents, at intermediate voltages (region II) by recombination currents, and at high voltage (region III) by the series resistance [40]. From Fig. 3 we can also see that the J-V plots of the P3HT:PbS solar cell differ from those of the P3HT:PCBM device by a less distinct region II, indicating the non-ideal dark *J-V* characteristics of the P3HT:PbS solar cells. From the fitting variables shown in Table II, the P3HT:PbS solar cells show an ideality factor much larger than 2, compared to 1.8 for the reference P3HT:PCBM solar cell. In addition, the P3HT:PbS solar cells show a much higher dark saturation current density J_0. It has been reported that one of the

attributes of the non-ideal behavior of the dark *J-V* characteristics of silicon solar cells is a large recombination current, often indicated by an ideality factor larger than 2. In these silicon solar cells the edge regions or crystal defects like grain boundaries have been shown to be the major source of the recombination [43].

TABLE II. Diode parameters obtained from the current density-voltage (*J-V*) characteristics in the dark of the P3HT:PbS QDs solar cells (ITO/PEDOT:PSS/P3HT:PbS QDs/Ca/Ag). The parameters of each sample were averaged from dark *J-V* characteristics fitting of 3 different cells. *: Integrated planar-bulk-heterojunction structure: ITO/PEDOT:PSS/P3HT(5-10 nm)/P3HT:PbS/Ca/Ag (*cfr. infra*)

Samples	Acceptor loading[a]	t (nm)	$R_s \cdot A$ ($\Omega \cdot cm^2$)	$R_{sh} \cdot A$ ($\Omega \cdot cm^2$)	J_0 (A/cm^2)	n
P3HT:PbS-OAm	60	100	14±4	$(0.8\pm0.4)\times10^3$	$(6.7\pm2.7)\times10^{-4}$	7.6±0.6
P3HT:PbS-OT	60	90	22±6	$(8.5\pm2.3)\times10^2$	$(8.4\pm1.7)\times10^{-3}$	8.7±1.9
P3HT:PbS-AA	60	110	20±5	$(1.1\pm0.6)\times10^4$	$(1.2\pm0.5)\times10^{-4}$	7.2±0.4
P3HT :PbS-BDT	60	180	33±0.7	$(6.7\pm2.5)\times10^5$	$(3.5\pm2.2)\times10^{-6}$	4±0.6
	75	160	78±22	$(6.4\pm1.6)\times10^3$	$(2.4\pm0.9)\times10^{-5}$	6±2.4
	90	160	17.4±8	$(4.4\pm0.6)\times10^3$	$(1.4\pm0.3)\times10^{-4}$	7±1.7
	100	140	106±41	$(1.6\pm0.9)\times10^5$	$(1.8\pm0.6)\times10^{-5}$	3±0.5
	90*	140	27±7	$(1.4\pm0.7)\times10^4$	$(6.2\pm2.8)\times10^{-5}$	3.8±0.3
P3HT:PCBM	50	100	11±2	$(3.6\pm1.8)\times10^5$	$(5.8\pm1.5)\times10^{-9}$	1.8±0.02

[a]The acceptor loading corresponds to the ratio of the weight of PbS QDs to the sum of the weight of PbS QDs and P3HT

When the solar cell device is under illumination at the conditions of an open circuit *(J=0)* and with the assumption that $R_{sh} >> R_s$, the open circuit voltage can be expressed as [44]:

$$Voc = \frac{nkT}{q} \ln\left(\frac{J_{SC}}{J_0} + 1\right) \quad (2)$$

In general, J_0 can be considered a direct estimate of the efficiency of recombination, which is a fundamental process determining V_{oc} of the device [44]. This is consistent with our observation that the lower V_{oc} of the P3HT:PbS solar cells is correlated with a high dark saturation current. When BDT was used to replace long OLA ligand in P3HT:PbS, the V_{oc} increases compared to the case where the other ligands were used. This is most probably due to an increase of short-circuit current J_{sc} and not to a decrease of recombination efficiency as the values of J_0 of the cells where the P3HT:PbS blend is treated with BDT are still quite high. The ideality factor is also

another important indicator of the recombination efficiency [45]. However, as the ideality factor, determined from the slope of the exponential regime of the dark *J-V* characteristics on a semi-logarithmic plot, is defined as $n = \left(\frac{kT}{q} \frac{\partial \ln J}{\partial V} \right)^{-1}$ and as also the series and shunt resistances influence the dependence of *J* on *V*, it is difficult to attribute the changes in the measured ideality factor to changes in shunt or series resistance on one hand or to changes of the recombination efficiency on the other hand [45-46].

The low FF observed for P3HT:PbS solar cell devices (see Table I) can be attributed to a relatively high series resistance and a low shunt resistance (see Table II). For the cells with BDT treated active layers and comparable thickness, the increase of the PbS loading seems to systematically decrease the shunt resistance. Current losses in the solar cells by the presence of a shunt resistance are typically due to the current leakage from the edge of the cell, from pinholes in the film or to trapping of charge carriers in deep traps [47]. It has been reported by Tan *et al.* [48] that the low shunt resistance in solar cells with a bulk heterojunction of a conjugated polymer and semiconductor QDs arose from the shunt contact between the electron transporting QDs and the ITO/PEDOT:PSS anode. They obtained an increase of the shunt resistance and the device performance when a thin layer (10 nm) of P3HT was inserted underneath the P3HT:PbSe blend layer. Indeed, as shown in Table II, when we adopted a similar structure (ITO/PEDOT:PSS/P3HT(5-10 nm)/P3HT:PbS/Ca/Ag), namely the integrated planar-bulk-heterojunction structure, the shunt resistance is increased while J_0 is decreased. This resulted in an improvement of the PCE to 1% (J_{sc}=7.1 mA/cm^2, V_{oc}=0.42 V and FF=34%). Furthermore as shown in Table S3[32] increasing the thickness of the active layer increased R_{sh} and decreased J_0.

It should be noted that PbS QDs-only solar cells show a higher shunt resistance and lower J_0 compared to solar cells with P3HT:PbS-BDT at a loading of 90 % suggesting that morphological effects also play a role in the shunt resistance. The solubility of the QDs in conjugated polymers is in general lower than that of PCBM , leading to a more extensive phase separation in the former case especially at high concentration of PbS QDs[1]. It has been reported that a good interfacial morphology can prevent current leakage and surface recombination [47]. Therefore, further tailoring the polymer/QDs interface at the nanoscale is very important to further improve the efficiency of polymer/QDs solar cells.

C Effect of the size of the PbS QDs

As a major difference with the best solar cells with a P3HT:PbS bulk-heterojunction reported up to now [19] and which have a PCE of 0.01 % resides in the size of the QDs we wanted to compare our results explicitly with hose of P3HT:PbS bulk-heterojunctions with larger PbS QDs prepared under identical conditions. Therefore we also measured the *J-V* characteristics of a device using larger QDs. As shown in Fig. S1[32], these QDs were estimated to have diameter of 3.5 and 4.4 nm (band-gap 1.18 and 0.99 eV), respectively. These devices show a very low PCE (<0.01%) even for a higher concentration of PbS QDs (see table S2[32]). However, one should note that these PbS QDs were obtained from a different source (see experimental details). Hence further studies are still needed in order to confirm that the low PCE is due to a size effect rather than to in the surface properties of the PbS QDs.

IV CONCLUSIONS

In conclusion, we report the fabrication of hybrid bulk heterojunction solar cell containing P3HT and small PbS QDs. Different approaches of the surface modification of the QDs, namely solution-phase and post-deposition ligand exchange, have been performed. Decrease of the size of the QDs, control of the PbS QDs concentration, post-deposition exchange of the OLA ligand to a bifunctional-linker molecule of BDT and the insertion of a thin layer of P3HT underneath of P3HT:PbS blends, which led to an increase of the shunt resistance, gave rise to a significant improvement of the photovoltaic energy conversion to 1% compared to the bench mark system with a bulk-heterojunction of P3HT:PbS QDs capped with AA ligands.[19] In addition, devices with larger QDs (3.5 and 4.4 nm) showed a very low PCE (<0.01%), although further studies are still needed to confirm if the performance is exclusively due to a size effect of the QDs. Dark *J-V* characteristics of the reference P3HT:PCBM and the P3HT:PbS blends were measured to gain understanding on the performance losses and the still limited device efficiency. In contrast to the bench mark device with P3HT:PCBM, the P3HT:PbS QDs solar cells showed a non-ideal behavior of the dark *J-V* curve which is characterized by an ideality factor much larger than 2. The analysis of the *J-V* curves also showed that further improvement of the performance of the P3HT:PbS bulk-heterojunction devices requires a reduction of the leakage current and the recombination losses to values typical for solar cells based on P3HT:PCBM bulk-heterojunctions.

ACKNOWLEDGMENTS

This work was supported by the IMEC Leuven (PhD grant to Y.F.) and by the EU through FP7 People Herodot (grant 214954). We are indebted to the research council of KULeuven through GOA 2006/3, 2011/2 and to Belspo through IAP VI/27 en IAP VII/05.

[1] A.J. Moulé, L. Chang, C. Thambidurai, R. Vidu, and P. Stroeve, J. Mater. Chem. **22**, 2351 (2012).

[2] J.-S. Lee, M. V Kovalenko, J. Huang, D.S. Chung, and D. V Talapin, Nat. Nanotechnol. **6**, 348 (2011).

[3] J. Tang and E.H. Sargent, Adv. Mater. **23**, 12 (2011).

[4] C. Smith and D. Binks, Nanomaterials **4**, 19 (2013).

[5] J. Tang, K.W. Kemp, S. Hoogland, K.S. Jeong, H. Liu, L. Levina, M. Furukawa, X. Wang, R. Debnath, D. Cha, K.W. Chou, A. Fischer, A. Amassian, J.B. Asbury, and E.H. Sargent, Nat. Mater. **10**, 765 (2011).

[6] A.A.R. Watt, D. Blake, J.H. Warner, E.A. Thomsen, E.L. Tavenner, H. Rubinsztein -Dunlop, and P. Meredith, J. Phys. D. Appl. Phys. **38**, 2006 (2005).

[7] Z. Wang, S. Qu, X. Zeng, C. Zhang, M. Shi, F. Tan, Z. Wang, J. Liu, Y. Hou, F. Teng, and Z. Feng, Polymer (Guildf). **49**, 4647 (2008).

[8] B. Sun and N.C. Greenham, Phys. Chem. Chem. Phys. **8**, 3557 (2006).

[9] C. Piliego, M. Manca, R. Kroon, M. Yarema, K. Szendrei, M.R. Andersson, and M.A. Loi, J. Mater. Chem. **22**, 24411 (2012).

[10] J. Seo, M.J. Cho, D. Lee, a N. Cartwright, and P.N. Prasad, Adv. Mater. **23**, 3984 (2011).

[11] K.M. Noone, E. Strein, N.C. Anderson, P.-T. Wu, S. a Jenekhe, and D.S. Ginger, Nano Lett. **10**, 2635 (2010).

[12] K.M. Noone, N.C. Anderson, N.E. Horwitz, A.M. Munro, A.P. Kulkarni, and D.S. Ginger, ACS Nano **3**, 1345 (2009).

[13] A. Guchhait, A.K. Rath, and A.J. Pal, Sol. Energy Mater. Sol. Cells **95**, 651 (2011).

[14] B. Hyun, Y. Zhong, A.C. Bartnik, L. Sun, H.D. Abrun, F.W. Wise, J.D. Goodreau, J.R. Matthews, T.M. Leslie, and N.F. Borrelli, ACS Nano **2**, 2206 (2008).

[15] P. Siders and R. A. Marcus, J. Am. Chem. Soc. 103, 748.

[16] R.A. Marcus, J. Chem. Phys. **81**, 4494 (1984).

[17] S. Zhang, P.W. Cyr, S.A. McDonald, G. Konstantatos, and E.H. Sargent, Appl. Phys. Lett. **87**, 233101 (2005).

[18] S. Hinds, L. Levina, E.J.D. Klem, G. Konstantatos, V. Sukhovatkin, and E.H. Sargent, Adv. Mater. **20**, 4398 (2008).

[19] J. Seo, S.J. Kim, W.J. Kim, R. Singh, M. Samoc, A.N. Cartwright, and P.N. Prasad, Nanotechnology **20**, 095202 (2009).

[20] K.M. Noone, S. Subramaniyan, Q. Zhang, G. Cao, S.A. Jenekhe, and D.S. Ginger, J. Phys. Chem. C **115**, 24403 (2011).

[21] M.T. Dang, L. Hirsch, and G. Wantz, Adv. Mater. **23**, 3597 (2011).

[22] Y. Liang, Z. Xu, J. Xia, S.-T. Tsai, Y. Wu, G. Li, C. Ray, and L. Yu, Adv. Mater. **22**, E135 (2010).

[23] Z. He, C. Zhong, X. Huang, W.-Y. Wong, H. Wu, L. Chen, S. Su, and Y. Cao, Adv. Mater. **23**, 4636 (2011).

[24] H. Zhong, Z. Li, F. Deledalle, E.C. Fregoso, M. Shahid, Z. Fei, C.B. Nielsen, N. Yaacobi-Gross, S. Rossbauer, T.D. Anthopoulos, J.R. Durrant, and M. Heeney, J. Am. Chem. Soc. **135**, 2040 (2013).

[25] I. Moreels, K. Lambert, D. Smeets, D. De Muynck, T. Nollet, J.C. Martins, F. Vanhaecke, A. Vantomme, C. Delerue, G. Allan, and Z. Hens, ACS Nano **3**, 3023 (2009).

[26] Y. Justo, I. Moreels, K. Lambert, and Z. Hens, Nanotechnology **21**, 295606 (2010).

[27] M. Law, J.M. Luther, Q. Song, B.K. Hughes, C.L. Perkins, and A.J. Nozik, J. Am. Chem. Soc. **130**, 5974 (2008).

[28] T. Hanrath, D. Veldman, J.J. Choi, C.G. Christova, M.M. Wienk, and R. a J. Janssen, ACS Appl. Mater. Interfaces **1**, 244 (2009).

[29] A. Sashchiuk, L. Amirav, M. Bashouti, M. Krueger, U. Sivan, and E. Lifshitz, Nano Lett. **4**, 159 (2004).

[30] Y. Firdaus, A. Khetubol, S. Kudret, H. Dilien, W. Maes, L. Lutsen, D. Vanderzande, and M. Van der Auweraer, Photonics Sol. Energy Syst. IV **8438**, 84381G (2012).

[31] Y. Firdaus, S. Kudret, A. Khetubol, W. Maes, L. Lutsen, B. Li, W. Frederickx, S. Flamée, W. Vanderlinden, Z. Hens, S. De Feyter, D. Vanderzande, and M. Van der Auweraer, "Role of structural order on optical properties, film morphology and hole transport of Poly(3-hexylthiophene) (P3HT) and P3HT:PbS blends" unpublished (2014) (unpublished.

[32] See supplementary material at link here for the absorption spectra of PbS QDs of different size, the weight percent and volume percent calculation of the components of the P3HT:PbS blends, the device performance of P3HT:PbS blend devices for PbS QDs with diameter 3.5 and 4.4 nm and the thickness dependence of the solar cell parameters [Supplementary Material].

[33] F.C. Spano, J. Chem. Phys. **122**, 234701 (2005).

[34] F.C. Spano, Chem. Phys. **325**, 22 (2006).

[35] M.C. Scharber, D. Mühlbacher, M. Koppe, P. Denk, C. Waldauf, A.J. Heeger, and C.J. Brabec, Adv. Mater. **18**, 789 (2006).

[36] A. Gocalińska, M. Saba, F. Quochi, M. Marceddu, K. Szendrei, J. Gao, M. a. Loi, M. Yarema, R. Seyrkammer, W. Heiss, A. Mura, and G. Bongiovanni, J. Phys. Chem. Lett. **1**, 1149 (2010).

[37] C.J. Brabec, F. Padinger, N.S. Sariciftci, and J.C. Hummelen, J. Appl. Phys. **85**, 6866 (1999).

[38] Y. Liu, M. Gibbs, J. Puthussery, S. Gaik, R. Ihly, H.W. Hillhouse, and M. Law, Nano Lett. **10**, 1960 (2010).

[39] Y. Firdaus, R. Miranti, E. Fron, A. Khetubol, H. Borchert, J. Parisi, and M. Van der Auweraer, "Charge separation dynamics in P3HT/PbS hybrid solar cells" (2014) (unpublished).

[40] J.D. Servaites, M.A. Ratner, and T.J. Marks, Energy Environ. Sci. **4**, 4410 (2011).

[41] W. Yoon, J. E. Boercker, M. P. Lumb, D. Placencia, E. E. Foos, and J. G. Tischler, Sci. Rep. 3, 2225 (2013).

[42] W.T.V. William H. Press , Brian P. Flannery, Saul A. Teukolsky, *Numerical Recipes in C*, 2nd ed. (Cambridge University Press, 1992).

[43] O. Breitenstein, J. Bauer, a. Lotnyk, and J.-M. Wagner, Superlattices Microstruct. **45**, 182 (2009).

[44] B. Qi and J. Wang, J. Mater. Chem. **22**, 24315 (2012).

[45] T. Kirchartz, F. Deledalle, P.S. Tuladhar, J.R. Durrant, and J. Nelson, J. Phys. Chem. Lett. **4**, 2371 (2013).

[46] G.A.H. Wetzelaer, M. Kuik, M. Lenes, and P.W.M. Blom, Appl. Phys. Lett. **99**, 153506 (2011).

[47] B. Qi and J. Wang, Phys. Chem. Chem. Phys. **15**, 8972 (2013).

[48] Z. Tan, T. Zhu, M. Thein, S. Gao, A. Cheng, F. Zhang, C. Zhang, H. Su, J. Wang, R. Henderson, J. Hahm, Y. Yang, and J. Xu, Appl. Phys. Lett. **95**, 063510 (2009).

Supporting information

Enhancement of the photovoltaic performance in P3HT: PbS hybrid solar cells using small size PbS quantum dots

Yuliar Firdaus[1], Erwin Vandenplas[2], Yolanda Justo[3], Robert Gehlhaar[2], David Cheyns[2], Zeger Hens[3], Mark Van der Auweraer[1,*)]

[1] *Laboratory of Photochemistry and Spectroscopy, Division of Molecular Imaging and Photonics, Chemistry Department, KULeuven, Celestijnenlaan 200F, B2404, B-3001 Leuven, Belgium*

[2] *Imec vzw, Kapeldreef 75, B-3001 Leuven, Belgium*

[3] *Physical Chemistry Laboratory, Ghent University, Krijgslaan 281-S3, 9000, Gent, Belgium*

[*)] Author to whom correspondence should be addressed. Electronic mail: mark.vanderauweraer@chem.kuleuven.be.

Absorption of PbS QDs

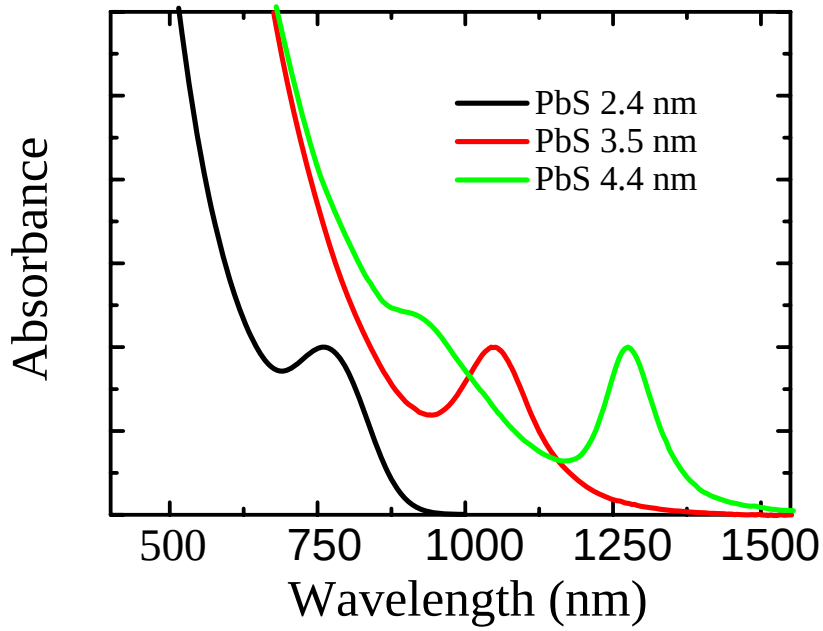

FIG. S1. Normalized absorption spectra of PbS QDs of different diameters dissolved in toluene. The legend shows the diameter of the QDs estimated according to their optical bandgap as derived from the maximum of the excitonic band.

Weight percent to volume percent calculation of P3HT:PbS blends

Assuming that the PbS QDs are not capped by ligands the weight and volume percent of PbS QDs in the P3HT:PbS blends amount to:

$$\text{wt\%} = 100\% \times \frac{w_{PbS}}{w_{PbS} + w_{P3HT}} \quad \text{(S1)}$$

$$\text{vol\%} = 100\% \times \frac{v_{PbS}}{v_{PbS} + v_{P3HT}} \quad \text{(S2)}$$

The weight % as determined by eq. S1 is called the "*loading*" contrary to the weight and volume % including the ligands as given by eq. S3 and S4, the calculation of which needs some assumptions. The loading can be determined directly from the amount of P3HT used to prepare the solutions and the volume and concentration of the QD solution

If the ligands are considered the volume percent of PbS QDs in P3HT:PbS blends becomes:

$$wt\% = \frac{w_{PbS}}{w_{PbS} + w_{P3HT} + w_{ligand}} \quad \text{(S3)}$$

$$\text{vol\%} = 100\% \times \frac{v_{PbS}}{v_{PbS} + v_{P3HT} + v_{ligand}} \quad \text{(S4)}$$

with $v_{P3HT} = w_{P3HT} / D_{P3HT}$; $v_{PbS} = N_{PbS} V_{1PbS}$; $v_{ligand} = w_{ligand} / D_{ligand}$ (here it is assumed that the density of the ligands in the blends is identical to their bulk density) where w_{PbS} and w_{ligand} are determined by:

$$w_{PbS} = N_{PbS} V_{1PbS} D_{PbS} ; \quad \text{eq. S5}$$

$$w_{ligand} = M_{ligand} \times \frac{N_{ligand}}{N_A} = M_{ligand} \times \frac{80 \times w_{PbS}}{N_A V_{1PbS} D_{PbS}} \quad \text{eq. S6}$$

v_{P3HT}: volume of P3HT (in cm^3)

v_{PbS}: volume of PbS (in cm^3)

v_{PbS}: volume of the ligands (in cm^3)

w_{P3HT}: weight of P3HT (in gram)

w_{PbS}: weight of PbS (in gram)

w_{ligand}: weight of the ligands (in gram)

D_{P3HT}: density of P3HT (1.15 g/cm^3)

D_{PbS}: density of PbS (7.61 g/cm^3)

D_{ligand}: density of the ligands (0.895, 0.782, 0.843, 1.049 and 1,24 g/cm^3 for OLA, OAm, OT, AA and BDT respectively)

M_{ligand}: Molar mass of the ligands (g/mol)

V_{1PbS}: Volume of a single PbS QD (7.235x10^{-21} cm^3 for PbS QDs with a diameter of 2.4 nm)

N_A: Avogadro constant

N_{PbS}: Number of PbS QDs, can be calculated from the known concentration of colloidal QDs (which is ~690 μM for the solution of PbS QDs with a diameter of 2.4 nm obtained from Evident Techology) and the volume of this solution used to prepare the blend solution

N_{ligand}: Total number of ligands on the PbS QDs (N_{ligand}=80N_{PbS}). This value is calculated knowing that that each QD is capped by ~80 ligands. . This ratio was estimated for a solution of PbS QDs capped by OLA using NMR spectra (using CH_2Br_2 as a concentration standard[1]). We also assumed that the ligand exchange replaced all the initial ligands of OLA which is a good estimate for BDT or OT.

TABLE S1 Weight and volume% of PbS QDs in P3HT:PbS blends.

% Loading	wt% (OLA ligand)	wt% (OT ligand)	wt% (OAm ligand)	w% (AA ligand)	wt% (BDT ligand)
60	42.6	49.5	50.6	55.2	49.8
75	49.7	59.3	60.8	67.7	59.7
90	55.8	68.3	70.3	79.6	68.8
100 %	59.5	74.0	76.3	87.4	74.5

% Loading	vol% (no ligand)	vol% (OLA ligand)	vol% (OT ligand)	vol% (OAm ligand)	vol% (AA ligand)	vol% (BDT ligand)
60	18	8.9	11.6	11.9	15.5	13.3
75	31	11.1	15.7	16.0	23.5	18.8
90	58	13.3	20.3	21.0	35.9	26.1
100 %	100	14.7	23.9	24.8	48.8	32.2

The loading is calculated by eq. S1 where the weight of PbS QDs is determined using eq. S5. The volume fraction estimated for the case when only the PbS core is considered (eq. S2) and when also the ligand are considered (eq. S4). The results in table S1 show that the volume fraction of the PbS core in the blends goes down as the ligands become larger (from BDT (8 non-hydrogen atoms) to OT (9 non-hydrogen atoms) and then to OLA (20 non-hydrogen atoms). In these calculations it was also assumed that ligand substitution occurred with 100 % efficiency.

Performance of devices of P3HT:PbS blend films for PbS QDs with a diameter of 3.5 nm and 4.4 nm

TABLE S2 Average photovoltaic performance values of P3HT:PbS treated with 1,4 benzenedithiol for PbS 3.5 nm and PbS 4.4 nm (*t*: thickness of the bulk heterojunction layer, J_{SC}: short circuit current, V_{OC}: open circuit voltage, FF: fill factor, Eff: energy efficiency).

d (nm)	PbS loading (%)	*t* (nm)	J_{sc} (mA/cm^2)	V_{oc} (V)	FF (%)	Eff (%)

3.5	60	120	0.83±0.05	0.04±0.006	26±2	$(8.5\pm1)\times10^{-3}$
	75	70	0.8±0.14	0.03±0.006	23±2	$(5\pm2)\times10^{-3}$
	90	100	1.5±0.02	0.01	12±5	$(2\pm0.7)\times10^{-3}$
4.4	60	105	0.63±0.08	0.05±0.007	27±2	$(8\pm2)\times10^{-3}$
	75	190	0.7±0.09	0.04±0.005	25±1.6	$(7\pm1)\times10^{-3}$
	90	200	0.8±0.1	0.03±0.007	27±2	$(6\pm2)\times10^{-3}$

Thickness dependence of the solar cell parameters

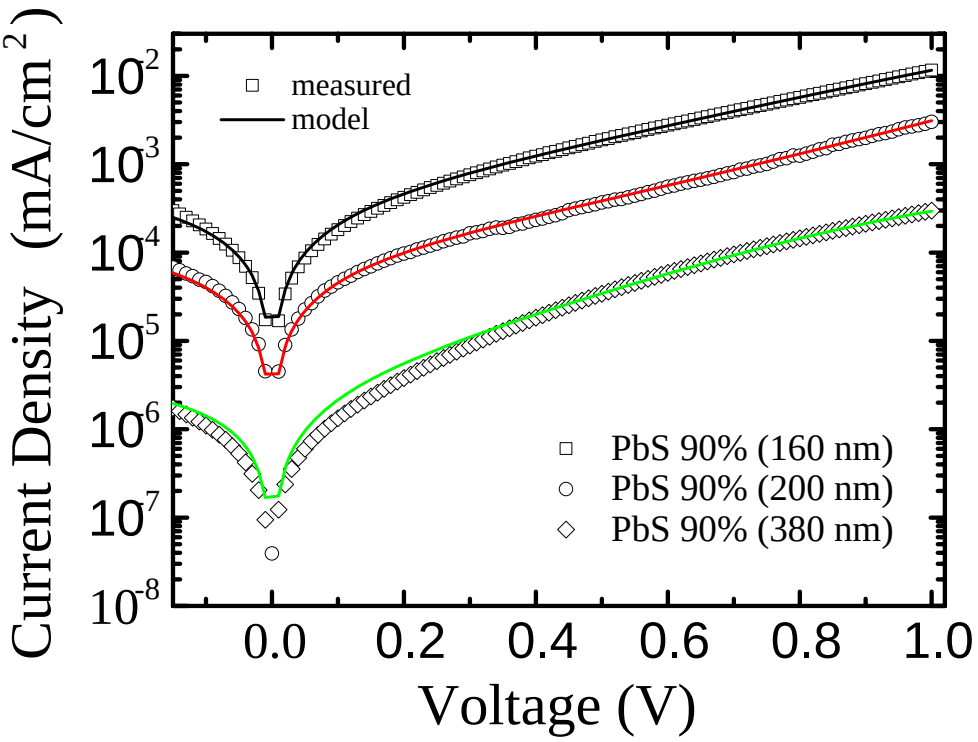

FIG. S2**.** Current density-Voltage (*J-V*) characteristics in the dark for P3HT:PbS-BDT 90% solar cells of different thickness with the following structure: ITO/PEDOT:PSS/active-layer/Ca/Ag

TABLE S3 Thickness dependence of the device performance of P3HT:PbS-BDT 90 wt% solar cells. The data were averaged over several cells of the same sample (7-12 cells).

Samples	t (nm)	J_{sc} (mA/cm^2)	V_{oc} (V)	FF (%)	Eff (%)
P3HT:PbS-BDT 90 wt%	160	7.2±0.1(7.2)	0.35±0.02(0.37)	33±0.8(34)	0.84±0.05(0.91)
	200	7.2±0.4(7.7)	0.35±0.04(0.38)	28.3±0.7(28.8)	0.72±0.1 (0.84)
	380	4±0.3(4.4)	0.34±0.03(0.36)	27.3±0.6(27.1)	0.37±0.05(0.43)

TABLE S4 Diode parameters obtained from the current density-voltage (*J*-*V*) characteristics in the dark of solar cells of P3HT:PbS-BDT 90 wt% with different thickness. The parameters of each sample were averaged from dark J-V characteristics for 3 different cells.

Samples	t (nm)	$R_s \cdot A$ ($\Omega \cdot$cm^2)	$R_{sh} \cdot A$ ($\Omega \cdot$cm^2)	J_0 (A/cm^2)	n
P3HT:PbS-BDT 90 wt%	160	17.4±8.1	$(4.4\pm0.6)\times10^{3}$	$(1.4\pm0.3)\times10^{-4}$	6.9±1.7
	200	45.1±10.9	$(8.2\pm6.5)\times10^{4}$	$(7.4\pm3.4)\times10^{-5}$	7.2±0.1
	380	122.2±60.6	$(1.9\pm1.6)\times10^{6}$	$(1.7\pm0.7)\times10^{-6}$	4.3±0.4

References

[1] I. Moreels, B. Fritzinger, J.C. Martins, and Z. Hens, J. Am. Chem. Soc. **130**, 15081 (2008).